ANALYSIS OF THE EQUATIONS OF HYPERSONIC FLOW AND THE SOLUTION OF THE CAUCHY PROBLEM

(ANALIZ URAVNENII GIPERZVUKOVYKH TECHENII I RESHENIE ZADACHI KOSHI)

PMM Vol.26, No.2, 1962, pp. 289-299

M.D. LADYZHENSKII
(Moscow)

(Received September 26, 1961)

The general equations of three-dimensional rotational hypersonic flow are investigated. A solution of the Cauchy problem is given, in which is noted the existence of infinite regions of determination of the solution. Comparison is made between an approximate solution of the Cauchy problem and the results of exact analytical and numerical solutions. The results of the work are used to determine internal hypersonic flows.

1. We consider the most general equations of three-dimensional rotational hypersonic flow. We take the equations, expressing steady isoenergetic flow of an ideal perfect gas, in the form

$$\operatorname{div}\left(1-\frac{V^2}{V_m^2}\right)^{\frac{1}{\varkappa-1}}\mathbf{V}=0, \qquad \operatorname{rot}\mathbf{V}\times\mathbf{V}=\frac{V_m^2-V^2}{2}\operatorname{grad}\sigma \tag{1.1}$$

$$\sigma=\ln\frac{p^{1/\varkappa}}{\rho}+\text{const}, \qquad \frac{V^2}{2}+\frac{\varkappa}{\varkappa-1}\frac{p}{\rho}=\frac{V_m^2}{2} \tag{1.2}$$

Here χ is the adiabatic index, $\mathbf{V}$ the velocity vector, V_m the maximum speed, σ the entropy function, p the pressure, and ρ the density. We will assume that the local Mach number $M \gg 1$; we write the velocity vector in the form

$$\mathbf{V}=V_m(1-\eta)\,\boldsymbol{\tau} \qquad (0<\eta\ll 1, \quad \boldsymbol{\tau}=1) \tag{1.3}$$

According to the Bernoulli equation

$$M=\sqrt{2}(1-\eta)\,[(\varkappa-1)\,\eta\,(2-\eta)]^{-1/2} \tag{1.4}$$

Substituting the expression (1.3) for the velocity $\mathbf{V}$ into (1.1), we obtain a system of quasilinear equations for η, σ and $\boldsymbol{\tau}$, to which must be added the relation $\boldsymbol{\tau} = 1$. The coefficients of this system consist of multiples of polynomials in η. In order to simplify the equations, we neglect in each polynomial all terms except the first, containing η to the lowest power; in other words, we neglect quantities of the order of $\eta \sim M^{-2}$ in comparison with unity in the coefficients of the equation for each derivative, while making no assumption about the magnitude of the derivative itself; as a result we obtain

$$\frac{1}{\varkappa-1}\frac{\partial \ln \eta}{\partial s} + \operatorname{div}\boldsymbol{\tau} = 0, \qquad \tau = 1$$
$$-\boldsymbol{\tau}\frac{\partial \eta}{\partial s} + \operatorname{grad}\eta \equiv \operatorname{grad}_n \eta = \eta \operatorname{grad}\sigma - \frac{\partial \boldsymbol{\tau}}{\partial s} \tag{1.5}$$

Here $\operatorname{grad}_n \eta$ indicates the component of the vector $\operatorname{grad}\eta$ perpendicular to the streamline, and $\partial/\partial s$ the derivative along the streamline.

Equations (1.5) are particularly simply expressed in a system of coordinates whose axes are directed respectively along the tangent to the streamline, the principal normal n, and the binormal n_1:

$$\frac{\partial \sigma}{\partial s} = 0, \qquad k + \frac{\partial \eta}{\partial n} - \eta\frac{\partial \sigma}{\partial n} = 0, \qquad \frac{\partial \eta}{\partial n_1} - \eta\frac{\partial \sigma}{\partial n_1} = 0 \tag{1.6}$$

where k is the curvature of the streamline.

After the solution of (1.5) the pressure and density are determined by finding σ from the simplified (for $\eta \ll 1$) Bernoulli equation. As a result we have

$$p = p_0(2\eta)^{\frac{\varkappa}{\varkappa-1}}, \qquad \rho = \rho_0(2\eta)^{\frac{1}{\varkappa-1}}, \qquad p = p_0(\sigma), \qquad \rho = \rho_0(\sigma) \tag{1.7}$$
$$\frac{\varkappa}{\varkappa-1}\frac{p_0}{\rho_0} = \frac{V_m^2}{2}$$

In view of (1.7), Equations (1.5) may be reduced to a system of equations very close to the ordinary equations of hydrodynamics:

$$\frac{d\mathbf{V}_m}{dt} + \frac{1}{\rho}\operatorname{grad}_n p = 0, \qquad \frac{d\ln\rho}{dt} + \operatorname{div}\mathbf{V}_m = 0$$
$$\mathbf{V}_m = V_m\boldsymbol{\tau}, \qquad \frac{d}{dt} = V_m\frac{\partial}{\partial s}, \qquad \frac{d\sigma}{dt} = 0 \tag{1.8}$$

Equations (1.8) differ from the Euler equations in that the velocity vector has a constant modulus, and in the momentum equation there appears instead of the pressure gradient its component perpendicular to the streamline.

Both forms of the equations - (1.5) and (1.8) - are equivalent. Below the equations are used primarily in the form (1.5), which is very useful for analysis.

2. In [1] it is shown that for plane and axisymmetric flows the properties of solutions of Equations (1.5) are essentially determined by one parameter K, which is equal to the product of a Mach number M_* characteristic of a given flow and the quantity ϑ characterizing the range of variation of the angle of inclination of the velocity vector.

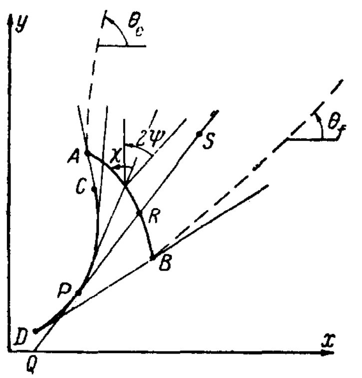

Fig. 1.

For flow past a slender body Equations (1.5) or (1.8) may be transformed into the equations of unsteady flow [2,3,4]. Then $K \sim 1$ always (the characteristic Mach number M_* is taken at any point of the disturbed flow, for example, at the leading edge of the body behind the shock wave), and the similarity parameter $K = M_\infty \vartheta$ introduced in [2] (where the subscript ∞ refers to the undisturbed stream) may vary from 1 to ∞. A similarity rule may be formulated for hypersonic flow past slender affinely-related bodies, using instead of K_∞ the parameter K and taking M_* at corresponding points for the flows being considered. Therefore K may be called the local similarity parameter for hypersonic flow.

For $K \ll 1$ a solution is obtained of the Cauchy problem, a knowledge of which, together with the solution of the mixed boundary problem, is necessary for the solution of internal flow. On the smooth arc AB (Fig.1) the quantities θ, η and σ are given as continuous and continuously differentiable functions of the arc length. For simplicity θ is assumed to be a monotonic function. On AB, by assumption, are satisfied the conditions

$$|\theta(A) - \theta(B)| \gg \sqrt{\max \eta}, \quad \chi - \psi > 0 \qquad (\psi = \tan^{-1}[(\varkappa - 1)\eta]^{1/2}) \quad (2.1)$$

where max η is the maximum value of η on AB, θ is the angle of inclination of the velocity vector with the axis of abscissae, χ the acute angle between the direction of the velocity vector and the tangent to AB, and ψ the Mach angle. The first condition (2.1) is equivalent to the requirement that $K \ll 1$ on AB. As is shown in Section 4, the second condition (2.1) is sufficient for the realization of the inequality $K \ll 1$ in the entire region of determination of the solution.* Here the streamlines

* By the region of determination of the solution of a given curvilinear segment (section of surface in the three-dimensional case) is under-

are, with an error of order K^{-2}, straight rays, and the solution of the Cauchy problem for plane ($\nu = 0$) and axisymmetric ($\nu = 1$) flow takes along each ray the form [1]

$$\eta = \eta_0 \left| \frac{r_0}{r} \right|^{\varkappa - 1} \left| \frac{r_0 + a}{r + a} \right|^{\nu(\varkappa - 1)}$$

$$\theta = \theta_0, \qquad \sigma = \sigma_0 \tag{2.2}$$

where subscript 0 indicates quantities on AB, and r and a denote respectively the distances (Fig. 1) measured from point P of the tangent of the ray with the envelope of rays CD to the point S under consideration and to the point Q of intersection of the ray with the axis of symmetry in axisymmetric flow.

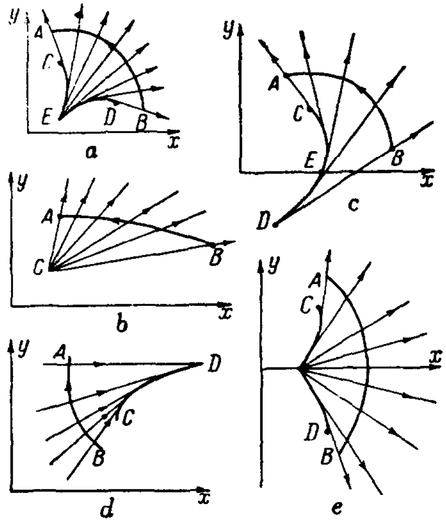

Fig. 2.

In view of the monotonic character of the variation of θ, the envelope CD lies on one side of AB. The direction of the velocity vector is assigned at each point of AB. If the region where the flow arises lies to the left of AB, then $r > 0$ when CD lies to the left (Figs. 2*a*, *b*, *c*), and correspondingly $r < 0$ when CD is to the right of AB (Fig. 2*d*). Furthermore, $a > 0$ when the envelope lies above the axis of symmetry (CE in Fig. 2*c*) and $a < 0$ for the segment DE in Fig. 2*c*. We draw the following conclusions with regard to the solution of (2.2).

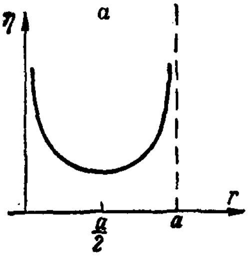

Fig. 3*a*

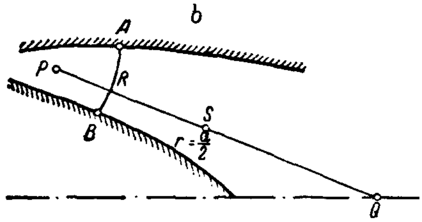

Fig. 3*b*

stood that region in which the solution of the Cauchy problem is completely determined by the assignment of Cauchy data on this segment (section of surface).

(1) The solution of (2.2) with the adopted accuracy coincides with the asymptotic solution, obtained previously by V.N. Gusev and M.D. Ladyzhenskii, of the problem of isentropic plane or axisymmetric efflux of a gas jet from an orifice into vacuum, according to which the flow at a great distance from the center O of the orifice tends asymptotically along each ray issuing from the point O to the flow from a certain plane or axisymmetric source with, generally speaking, intensity varying from ray to ray.

(2) In the case of Fig. 2*d* the value of η changes non-monotonically along a ray, having the character shown in Fig. 3*a*. Such a case can be realized for hypersonic flow in a channel with a central body (Fig. 3*b*).

(3) The solution of (2.2) is accurate at a sufficient distance from the envelope and the axis of symmetry, where η becomes infinite. This does not rule out, however, the case when the axis of symmetry is one of the rays in the solution of (2.2), as shown in Fig. 2*e*.

It is evident that in using the solution of (2.2) along the axis of symmetry in axisymmetric flow, one must set $a = 0$ in the solution.

(4) It is possible that simultaneously $\vartheta \ll 1$ and $K \gg 1$. Then with a relative error of order ϑ^2 Equations (1.5) or (1.8) can be transformed to the equations of unsteady flow, after which further simplification can be carried out in view of $K \gg 1$. The solution of (2.2) may thus also be built up from the theory of unsteady gas motion.

3. We investigate three-dimensional flows. In the case of flow past a slender body ($K \sim 1$) Equations (1.8) can be easily transformed into the equations of unsteady flow.

We consider the solution of the Cauchy problem. Let continuous and continuously differentiable functions τ, η and σ be given on a certain surface S. The following assumptions are made, analogous to (2.1):

(1) At least two of the three quantities ϑ_i ($i = 1, 2, 3$), characterizing the variation of the angle of the vector τ with the axes of a Cartesian coordinate system exceed η by an order of magnitude on S.

(2) The Mach cone issuing from each point of the surface S does not intersect that surface.

With these assumptions it follows from the last of Equations (1.5) that $\partial\tau/\partial s = 0$, that is, the streamlines are straight lines. If the surface is constructed for which these rays are the normals then the value of div τ is known to be twice the average curvature of this surface. In moving along a given ray, surfaces are intersected whose centers of curvature lie at the same points O_1 and O_2 for all the surfaces. Denoting the distance between these points by a, we obtain from the first of Equations (1.5) the solution in the form (2.2), where r and r_0 denote the distances from one of the centers of curvature to the point under consideration and the surface S respectively. The remarks 2-4 in Section 2 are extended to the general case.

4. For plane and axisymmetric flow we consider the question of the unbounded region of determination of the solution for $K \gg 1$. It is known that the solution of the Cauchy problem for a given arc segment AB, if it exists, is determined in a curvilinear triangle, one side of which is AB and the other two are characteristics of different families passing through the points A and B.

Assuming for simplicity that the flow is isentropic and that the envelope is concentrated into a point as in Fig. 2e (this last in the case of axisymmetric flow) we obtain the equation of the characteristics in the hodograph plane of θ (the angle of inclination of the velocity vector with the x-axis) and η

$$\pm\,\theta(1+\nu)+\frac{2}{\sqrt{\varkappa-1}}\sqrt{\eta}=\text{const} \tag{4.1}$$

where the plus and minus signs refer to characteristics of the first and second family respectively.

Using (2.2), it is possible to obtain from Equation (4.1) the characteristics in the physical plane.

The equations of the characteristics passing through the points A and B take the form (Fig. 1)

$$-\,\theta_a(1+\nu)+\frac{2\sqrt{\eta_a}}{\sqrt{\varkappa-1}}=-\,\theta_e(1+\nu),\quad \theta_b(1+\nu)+\frac{2\sqrt{\eta_b}}{\sqrt{\varkappa-1}}=\theta_f(1+\nu) \tag{4.2}$$

These expressions are written proceeding from the fact that the characteristics AE and BF in the physical plane do not intersect as $\eta\to 0$. In fact, from the first of Equations (2.1) it follows that

$$\theta_e-\theta_f=\theta_a-\theta_b-\frac{2}{\sqrt{\varkappa-1}\,(1+\nu)}\left(\sqrt{\eta_a}+\sqrt{\eta_b}\right)\gg\sqrt{\eta} \tag{4.3}$$

and the characteristic triangle is unclosed.* In the hodograph plane this

* The significance of the second of Equations (2.1) is now evident. With the breaking of their characteristics AE and BF come out beyond the boundary of the region in which the solution of (2.2) is constructed.

finds its reflection in the fact that the characteristics AE and BF, not intersecting, each the line of parabolic degeneracy $\eta = 0$ (Fig. 4).

Thus in the Cauchy problem there appears an infinite region of determination of the solution. This significant property of the class of hypersonic flows under consideration is preserved, as it is not difficult to verify, in the general case of three-dimensional rotational hypersonic flow.

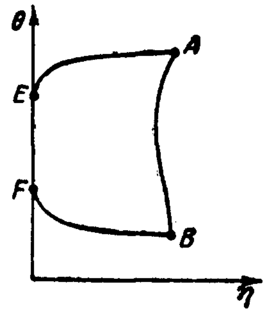

Fig. 4.

5. We pass to a consideration of the velocity in the hodograph plane. (The first similar investigation of hypersonic flow was carried out in [5], where a solution was constructed analogous to that used below.) Transition to the hodograph plane is feasible in the case of isentropic plane flow. In this case (cf. [6], for example) the Legendre potential Φ satisfies the equation

$$\frac{V^2}{1-V^2/c^2}\frac{\partial^2\Phi}{\partial V^2}+V\frac{\partial\Phi}{\partial V}-\frac{\partial^2\Phi}{\partial\theta^2}=0, \qquad \frac{V^2}{2}+\frac{c^2}{\varkappa-1}=\frac{V_m^2}{2} \tag{5.1}$$

where c is the speed of sound.

The transformation to Cartesian coordinates x, y is accomplished according to the equations

$$x=-\cos\theta\frac{\partial\Phi}{\partial V}+\frac{\sin\theta}{V}\frac{\partial\Phi}{\partial\theta}, \qquad y=-\sin\theta\frac{\partial\Phi}{\partial V}-\frac{\cos\theta}{V}\frac{\partial\Phi}{\partial\theta} \tag{5.2}$$

Introducing into Equations (5.1) the variable η (1.3) in place of V, we obtain after simplifications analogous to those carried out in Section 1

$$(\varkappa-1)\eta\frac{\partial^2\Phi}{\partial\eta^2}+\frac{\partial\Phi}{\partial\eta}-\frac{\partial^2\Phi}{\partial\theta^2}=0 \tag{5.3}$$

The equation obtained agrees with the equation [6] describing one-dimensional isentropic flow in the coordinates of enthalpy η and speed θ.

The transformation to the physical plane of x (the time) and y (the coordinate) is accomplished in the case of unsteady flow according to the equations, different from (5.2)

$$x=\frac{\partial\Phi}{\partial\eta}, \qquad y=\theta\frac{\partial\Phi}{\partial\eta}-\frac{\partial\Phi}{\partial\theta} \tag{5.4}$$

For equivalence of the two flows under consideration - hypersonic flow and unsteady flow - it is necessary to neglect in the expressions (5.2) quantities of order η in comparison with unity, and also suppose that θ is small, so that $\sin\theta \approx \theta$ and $\cos\theta \approx 1$. As a result Equations (5.2) are transformed into (5.4).

We take advantage of the exact solution of Equation (5.3) known [6] from the theory of unsteady flow, which can be constructed for $(3-\kappa)/(\kappa-1) = 2m$ where m is an integer, which embrace the case of practical interest of a monatomic gas ($m = 1$, $\kappa = 5/3$) and a diatomic gas ($m = 2$, $\kappa = 7/5$). This solution has the form

$$\Phi = \frac{\partial^{m-1}}{\partial\eta^{m-1}}\left\{\frac{1}{\sqrt{\eta}}\left[F_1\left(\theta+\frac{2\sqrt{\eta}}{\sqrt{\varkappa-1}}\right)+F_2\left(\theta-\frac{2\sqrt{\eta}}{\sqrt{\varkappa-1}}\right)\right]\right\} \tag{5.5}$$

where F_1 and F_2 are arbitrary functions determined by the boundary conditions.

We will use the equations of transformation to the physical plane in the form (5.4). Essentially an exact solution is found of the equations of unsteady flow for $K \gg 1$. (Cf. remark 4 in Section 2.)

In the hodograph plane the line AB (Fig. 4) is given by the equations $\eta = \Delta = \text{const}$, $\vartheta \geqslant \theta \geqslant 0$. On this line are given the physical coordinates

$$x = 0, \quad y = Y(\theta), \qquad y_0 \geqslant y \geqslant 0$$

After a series of computations which are omitted, the solution of the Cauchy problem for a monatomic gas ($\kappa = 5/3$) may be put in the form

$$x = -\frac{1}{2\eta}\sqrt{\frac{3\Delta}{2}}\,[Y(z_+)-Y(z_-)] + \frac{1}{8\eta^{3/2}}\sqrt{\frac{2}{3}}\int_{z_-}^{z_+}(\theta-\chi)\,Y(\chi)\,d\chi \tag{5.6}$$

$$y = \theta x + \frac{1}{2}\sqrt{\frac{\Delta}{\eta}}\,[Y(z_+)+Y(z_-)] + \frac{1}{4}\sqrt{\frac{2}{3\eta}}\int_{z_-}^{z_+}Y(\chi)\,d\chi$$

$$z_+ = \theta + \sqrt{6}\,(\sqrt{\eta}-\sqrt{\Delta}), \qquad z_- = \theta - \sqrt{6}\,(\sqrt{\eta}-\sqrt{\Delta})$$

The analogous expression for a diatomic gas ($\kappa = 7/5$) is

$$x = -\frac{3}{80\sqrt{10}}\,\frac{1}{\eta^{5/2}}\int_{z_-}^{z_+}Y(\chi)\,(\theta-\chi)^3\,d\chi + \frac{3(1+\Delta/\eta)}{8\sqrt{10}\,\eta^{3/2}}\int_{z_-}^{z_+}Y(\chi)\,(\theta-\chi)\,d\chi -$$

$$-\frac{\sqrt{10}\,\Delta}{4\eta^{3/2}}\,[Y(z_+)-Y(z_-)] \tag{5.7}$$

$$y = \theta x - \frac{3}{40\sqrt{10}}\,\frac{1}{\eta^{5/2}}\int_{z_-}^{z_+}Y(\chi)\,(\theta-\chi)^2\,d\chi + \frac{3+\Delta/\eta}{4\sqrt{10\eta}}\int_{z_-}^{z_+}Y(\chi)\,d\chi + \frac{\Delta}{2\eta}\,[Y(z_+)+Y(z_-)]$$

$$z_+ = \theta + \sqrt{10}\,(\sqrt{\eta}-\sqrt{\Delta}), \qquad z_- = \theta - \sqrt{10}\,(\sqrt{\eta}-\sqrt{\Delta})$$

The solutions (5.6) and (5.7) are determined in the hodograph plane in the region $AEFB$ (Fig. 4), which for $K^2 \sim \theta^2/\Delta \gg 1$ is bounded at $\eta = 0$ by a segment of the parabolic line. On this line Equation (5.3) experiences a parabolic degeneracy, the character of which is in principle different from the parabolic degeneracy of the Tricomi equation at $M = 1$. Equation (5.3) belongs to the second basic canonical form of equation exhibiting parabolic degeneracy (to the first form of which the Tricomi equation belongs).

In agreement with Section 4, in the physical plane the region of determination of the solution extends to infinity. The segment BF in the hodograph plane corresponds precisely to the limiting angle between the characteristics AE and BF at infinity (Fig. 1).

We expand the functions appearing in the expressions (5.6) that depend on $\theta \pm \sqrt{6}(\sqrt{\eta} - \sqrt{\Delta})$ in Taylor series in powers of $\sqrt{6}(\sqrt{\eta} - \sqrt{\Delta})$. We make a similar expansion in Equations (5.7) in powers of $\sqrt{10}(\sqrt{\eta} - \sqrt{\Delta})$. These expansions evidently have sense everywhere in the region $AEFB$. As a result we obtain

$$x = x_* [1 + f(\eta, \theta)], \qquad y = y_* [1 + g(\eta, \theta)] \tag{5.8}$$

where the quantities with subscript * have the form

$$x_* = \frac{dY}{d\theta}\left[\left(\frac{\Delta}{\eta}\right)^{3/2} - 1\right] \quad \text{for } \varkappa = \frac{5}{3} \tag{5.9}$$

$$x_* = \frac{dY}{d\theta}\left[\left(\frac{\Delta}{\eta}\right)^{5/2} - 1\right] \quad \text{for } \varkappa = \frac{7}{5} \tag{5.10}$$

$$y_* = \theta x_* + Y(\theta) \quad \text{for } \varkappa = \frac{5}{3} \text{ and } \frac{7}{5} \tag{5.11}$$

and f and g are determined from Equations (5.6) and (5.7). Equations (5.9) and (5.10) agree with the first of Equations (2.2), because with the accuracy adopted ($\cos\theta \approx 1$) one can write $Y'(\theta) = r_0$ and $x = r - r_0$, where r and r_0 have the same meaning as in Equation (2.2).

Equation (5.11) gives the stream lines as straight lines, in conformity with the second of Equations (2.2). The functions f and g appearing in Equations (5.8) characterize the accuracy with which the solution of the Cauchy problem obtained in Section 2 agrees with the exact solution determined by (5.6) and (5.7).

We rewrite the first terms of the expansions of these functions as series in powers of K, denoting the corresponding letters by subscript 1; for convenience of writing we introduce the notation $\Lambda = \sqrt{\eta/\Delta}$. For $\kappa = 5/3$ we have

$$f_1 = \frac{3}{5}\frac{Y'''\Delta}{Y'}\cdot\frac{(1-\Lambda)^3(1+3\Lambda+\Lambda^2)}{1-\Lambda^3} \tag{5.12}$$

$$g_1 = \frac{3\,(Y'''\theta\Delta/Y)(1-\Lambda)^3(1+3\Lambda+\Lambda^2)+5(Y''\Delta/Y)\,\Lambda^2(\Lambda-1)^2(2+\Lambda)}{5\,(Y'\theta/Y)(1-\Lambda^3)+5\Lambda^3} \tag{5.13}$$

and for $\kappa = 7/5$

$$f_1 = \frac{5}{42}\frac{Y'''\Delta}{Y'}\,\frac{(1-\Lambda)^3\,[6(\Lambda^4+1)+18\Lambda(\Lambda^2+1)+\Lambda^2]}{1-\Lambda^5} \tag{5.14}$$

$$g_1 = \frac{5}{42}\frac{Y'''\theta\Delta}{Y}\,\frac{(1-\Lambda)^3\,[6(\Lambda^4+1)+18\Lambda(\Lambda^2+1)+\Lambda^2]}{(Y'\theta/Y)(1-\Lambda^5)+\Lambda^5}+ \\ +\frac{Y''\Delta}{Y}\,\frac{\Lambda^2(\Lambda-1)^2\,[\Lambda^3+(4/3)\Lambda^2+(4/3)\Lambda+2/3]}{(Y'\theta/Y)[1-\Lambda^5]+\Lambda^5} \tag{5.15}$$

The expressions (5.12) to (5.15) contain as factors the quantities $Y''\Delta/Y$, $Y'''\theta\Delta/Y$, $Y'''/\Delta Y'$, which have the order $\Delta/\vartheta^2 \sim K^{-2}$.

Thus in confirmation of the results of Sections 2 and 4, with a relative error of order K^{-2}, the solution (2.2) may be used everywhere in the region of determination *AEFB* of the solution.

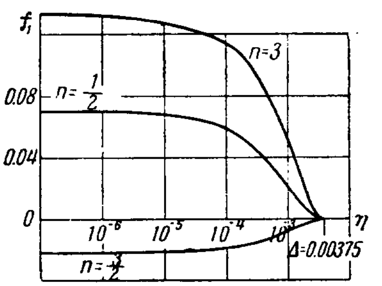

Fig. 5.

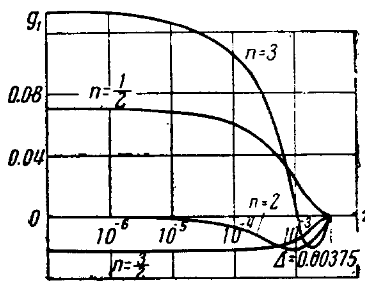

Fig. 6.

For a more detailed analysis of the accuracy, calculations of the quantities f_1 and g_1 as functions of η according to Equations (5.12) to (5.15) were introduced for values of Δ corresponding to $M = 20$, $\vartheta = 10^o$ for $\kappa = 5/3$ (Figs. 5 and 6) and also for $\vartheta = 20^o$ with $\kappa = 7/5$ (Figs. 7 and 8), which corresponds to K equation to 3.49 and 6.98 respectively. The function $Y(\theta)$ was put in powers in the form $Y = y_0(\theta/\vartheta)^n$. The calculations were carried out for values of $n = 1/2$, 1, 3/2, 2 and 3.

As $\eta \to 0$ the quantity f_1 tends to its limiting value, equal according to (5.12) to $9(n-1)(n-2)/10K^2$ for a monatomic gas, and according to (5.14) to $25(n-1)(n-2)/14K^2$ for a diatomic gas.

As follows from Figs. 5 and 7, the quantity f_1 varies monotonically as η increases from zero to its limiting value. For $n = 1$ and $n = 2$ we have $f \equiv 0$.

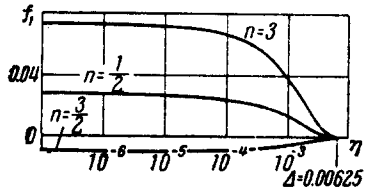

Fig. 7.

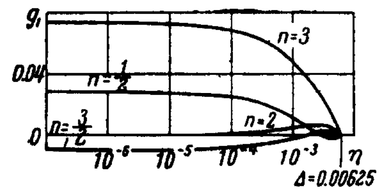

Fig. 8.

As $\eta \to$ the quantity g_1 (Figs. 6 and 8) tends to the same values as f_1. In contrast with f_1; g_1 may have a non-monotonic character. For $n = 1$, $g \equiv 0$. For $n = 2$ the function g_1 tends to zero as $\eta \to 0$.

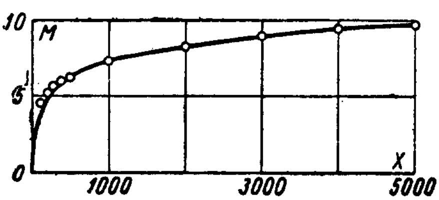

Fig. 9.

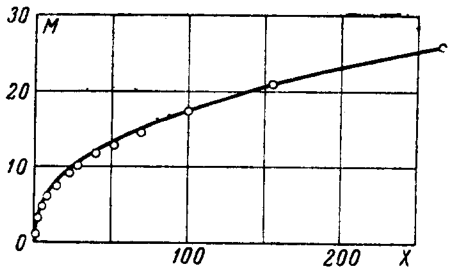

Fig. 10.

From the solution deduced it is possible to draw the conclusion that acceptable accuracy in the approximate solution of the Cauchy problem given above is obtained for $K \gtrsim 3.5$ in the case of a monatomic gas and $K \geqslant 7$ in the case of a diatomic gas.

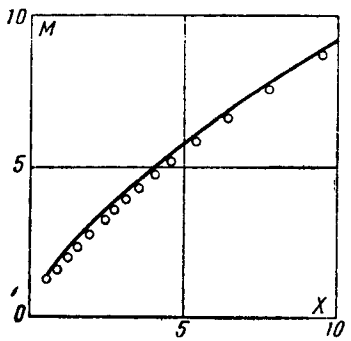

Fig. 11.

We give further a comparison (Figs. 9 to 11) of the solution obtained for the Cauchy problem with a numerical solution for the case of free efflux of gas from an orifice with a plane surface of transition.

From Equations (2.2) and (1.4) (writing henceforth $M = [(\kappa - 1)\eta]^{-1/2}$ in view of $\eta \ll 1$) and considering remark 3 in Section 2, the solution for the Mach number M along the axis of the jet assumes the form

$$M = M_0 \left(\frac{r}{r_0}\right)^{\frac{\varkappa-1}{2}(1+\nu)} \tag{5.16}$$

Figures 9 to 11 show the variation of Mach number M with the distance X along the axis of the jet, where $X = r/R$ and R is the radius or half height of the initial aperature through which the flow takes place.

Figure 9 corresponds to plane flow with $\kappa = 1.4$, the numerical solution (shown by a solid line) being taken from [7] and circles indicating values calculated from Equation (5.16). Figure 10 ($\kappa = 1.4$, with numerical data from [8] shown by circles, also in Fig. 11) and Fig. 11 ($\kappa = 1.6667$, with the numerical solution carried out by O.N. Katzkova at the Computing Center of the Academy of Sciences of the USSR) correspond to axisymmetric flow. The solid lines in Figs. 10 and 11 represent the relation (5.16). The constant values M_0 and r_0 in Equation (5.16) were determined for a certain $X = X_0$ coming from the numerical calculation. Adequate accuracy is attained already for $M_0 \gtrsim 4$. Indeed, the approximate solution of the Cauchy problem is well confirmed by the results of exact solutions and exact numerical calculations.

6. On the effect of viscosity. The conclusion regarding the appearance of an infinite region of determination of the solution may be

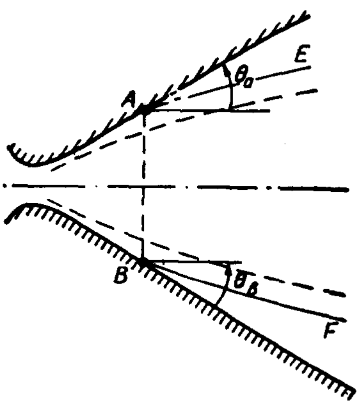

Fig. 12*a*.

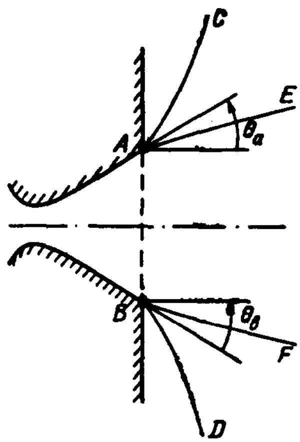

Fig. 12*b*.

used for an analysis of internal flow. We consider hypersonic flow in a nozzle as shown in Fig. 12*a**. In conformity with the construction of the

* A nozzle is considered in which the course of the flow proceeds without a subsequent rectilinear flow. The construction of the contour of a hypersonic nozzle in which there exists a partial rectilinear flow

solution for sufficiently large values of the number M on a certain line AB (such that on AB the condition $K \gg 1$ is satisfied) the flow in the nozzle is completely determined within an infinite region of determination of the solution $AEFB$ by giving the initial portion AB at the left. The difference between the limiting semi-angle $0.5(\theta_e - \theta_f)$ and the semi-angle of the nozzle on the line AB $0.5(\theta_a - \theta_b)$ is determined from Equation (4.3), which may be rewritten, assuming that $\theta_a = -\theta_b = \theta$ and $\theta_e = -\theta_f = \theta'$ and introducing the Mach number M_a at the point A, as

$$\theta - \theta' = \frac{2}{(\varkappa - 1)(1 + \nu)} \frac{1}{M_a} \tag{6.1}$$

For example, for an axisymmetric nozzle with $M_a = 10$ the difference between θ and θ' amounts to 14° for $\kappa = 1.4$ and 8.5° for $\kappa = 1.667$.

On the assumption that dissipative processes are absent, which was made everywhere up to now, the flow in the region $AEFB$ remains the same if the contour of the nozzle to the right of AB is changed, as indicated in Fig. 12*b*, so that beyond the line AB there exists flow into a vacuum.

However in internal hypersonic flow, on account of the great rarefaction, the effects of viscosity and heat conduction, as a rule, are very significant. It can be asserted that these effects will manifest themselves substantially differently in the cases of the flow of Figs. 12*a* and 12*b*. In the first case the boundary layer forming on the walls (dotted in Fig. 12*a*) may, for a sufficiently long nozzle, penetrate the region $AEFB$ and consequently alter the flow.

In the second case the processes of dissipation for flow into a vacuum are not connected with the appearance of a boundary layer.

Through the boundaries AC and BD of the jet in Fig. 12*b* there is no transfer of momentum and heat to the surrounding space, which is a vaccum, and therefore the total momentum and energy of the jet is preserved despite the presence of dissipative processes. There simply arises an irreversible transformation of mechanical into thermal energy, analogous to that occurring in a shock wave.

It may be expected that the effect of viscosity and heat conduction will much more strongly influence the flow of Fig. 12*a* than the case of

---

was carried out by A.A. Nikol'skii in a report at the All-Soviet Congress on Theoretical and Applied Mechanics from January 27 to February 3, 1960.

Fig. 12*b**. Nevertheless, dissipative processes limit the application of the solution (2.2) of the equations for an ideal gas also in the second case. In order to delimit the region of applicability of the indicated solution, we assume that in the infinite region of determination *AEFB* of the solution there takes place hypersonic flow from a source (in the actual general case the flow is obviously close to the flow from a source), for which Equation (2.2) is valid if we suppose that quantities with subscript 0 are constant in the whole region and $a = 0$. Expressing the parameters of the source in terms of the corresponding parameters at the critical section of the nozzle, denoted below by subscript *, we have for the radial component of velocity u and the other quantities in (1.7)

$$u = V_m\left[1-(\varkappa+1)^{-1}\left(\frac{\varkappa-1}{\varkappa+1}\right)^{(\varkappa-1)/2}\left(\frac{r_*}{r}\right)^{(\varkappa-1)(1+\nu)}\right]$$

$$p = p_*\left(\frac{\varkappa-1}{\varkappa+1}\right)^{\varkappa/2}\left(\frac{r_*}{r}\right)^{\varkappa(\nu+1)}, \qquad \rho = \rho_*\left(\frac{\varkappa-1}{\varkappa+1}\right)^{1/2}\left(\frac{r_*}{r}\right)^{1+\nu} \tag{6.2}$$

$$T = T_*\left(\frac{\varkappa-1}{\varkappa+1}\right)^{(\varkappa-1)/2}\left(\frac{r_*}{r}\right)^{(\varkappa-1)(\nu+1)}, \qquad M = \left(\frac{\varkappa+1}{\varkappa-1}\right)^{(\varkappa+1)/4}\left(\frac{r}{r_*}\right)^{(\nu+1)(\varkappa-1)/2}$$

where T is the temperature, the radius vector r is reckoned from the center of the critical section, and r_* is the radius of the critical section.

We will assume that the Prandtl number is constant, and furthermore assume a power-law dependence of the coefficient of viscosity μ upon temperature in the form $\mu = \mu_*(T/T_*)^n$. We substitute the expressions (6.2) into the Navier-Stokes equations and form the ratio of the largest viscous terms to the convective quantities

$$\left|\frac{\mu u/r^2}{\rho u u'}\right| = \left|\frac{\mu}{\rho u' r^2}\right| = \frac{1}{R} \leqslant \varepsilon \tag{6.3}$$

Here R indicates the local Reynolds number, and ε characterizes the required accuracy (in any case $\varepsilon \leqslant 0.1$). Equation (6.3) permits determination of the distance, which we denote by r^0, at which viscosity manifests itself, and of the corresponding value of the Mach number M (which we denote by M^0).

---

* It is understood that all that is said above is valid also in the case that outflow takes place (Fig. 12*b*) into a medium with a finite pressure p. It is only necessary that the pressure on the line *AB* be many times greater than p. Then the previous reasoning remains valid so long as the pressure in the jet does not become close to p.

Using Equations (6.2), we obtain

$$\frac{r^\circ}{r_*} \leqslant \left(\frac{\varkappa-1}{\varkappa+1}\right)^\alpha (\varepsilon R_*)^\beta, \qquad M^\circ \leqslant \left(\frac{\varkappa-1}{\varkappa+1}\right)^\gamma (\varepsilon R)^\delta \tag{6.4}$$

where R_* is the Reynolds number calculated for the characteristic parameters in the critical section, determined by the expression

$$R_* = \frac{\rho_* u_* r_* (\nu+1)}{\mu_*}$$

$$\alpha = \frac{\varkappa+1-(\varkappa-1)n}{2[(\varkappa-1)(1+\nu)(1-n)+\nu]}, \qquad \beta = \frac{1}{(\varkappa-1)(1+\nu)(1-n)+\nu} \tag{6.5}$$

$$\gamma = \frac{2n(\varkappa-1)(1+\nu)-(\varkappa+1)\nu}{4[(\varkappa-1)(1+\nu)(1-n)+\nu]}, \qquad \delta = \frac{(\varkappa-1)(1+\nu)}{2[(\varkappa-1)(1+\nu)(1-n)+\nu]}$$

(n is the power-law exponent in the expression for μ).

As analysis of the expression (6.4) shows, viscosity may become significant for some $r^\circ < \infty$ if $n < n^\circ$, where $n^\circ = 1$ for plane flow and $n^\circ = 1 + 0.5(\kappa - 1)^{-1}$ for axisymmetric flow. In plane flow even for $n < n^\circ$ the values of M° are so large that practically the limitation (6.4) is immaterial. For example, with $n = 0.7$, $\kappa = 1.4$ $\varepsilon R_* = 10^2$, we obtain for M° a value ~ 3000. In the case of axisymmetric flow a regime of flow may be encountered where viscosity significantly limits the application of the solution (2.2).

Values of M°

n	$\varkappa$	εR_*			
		10^2	10^3	10^4	10^5
0.75	1.67	12.0	38.0	120.7	383.3
	1.4	7.3	15.7	33.7	72.6
	1.2	5.5	8.4	12.8	19.4
0.5	1.67	8.4	21.0	53.0	133.5
	1.4	6.7	12.9	24.8	48.0
	1.2	5.3	7.8	11.4	16.7

We illustrate these resulting values of M° for two values of n.

As follows from the table, as κ and n decrease, which ordinarily accompanies an increase in temperature, the effects of viscosity and heat conduction increase. For $r > r^\circ$, when dissipative processes are significant, the flow is described by the Navier-Stokes equations, and the solution (2.2) is inapplicable.

The author would like to thank A.A. Nikolskii for discussion of this work.

BIBLIOGRAPHY

1. Ladyzhenskii, M.D., O techeniiakh gaza s bol'shoi sverkhzvukovoi skorost'iu (On gas flow at high supersonic speed). *Dokl. Akad. Nauk SSSR* Vol. 134, No. 2, 1960.

2. Tsien, H.S., Similarity laws of hypersonic flow. *J. Math. Phys.* Vol. 25, No. 3, 1946.

3. Hayes, W.D., On hypersonic similitude. *Quart. J. Appl. Math.* Vol. 5, No. 1, 1947.

4. Il'iushin, A.A., Zakon ploskikh sechenii v aerodinamike bol'shikh sverkhzvukovykh skorostei (The law of plane sections in the aerodynamics of high supersonic speeds). *PMM* Vol. 20, No. 6, 1956.

5. Fal'kovich, S.V., Ploskoe dvizhenie gaza pri bol'shikh sverkhzvukovykh skorostiakh (Plane motion of gas at high supersonic speed). *PMM* Vol. 11, No. 4, 1947.

6. Landau, L.D. and Lifshits, E.M., *Mekhanika sploshnykh sred (Mechanics of Continuous Media)*. GITTL, 1957.

7. Shapiro, A., *The Dynamics and Thermodynamics of Compressible Fluid*, I. Ronald Press, 1953.

8. Katskova, O.N. and Shmyglevskii, Iu.D., Osesimmetrichnoe sverkhzvukovoe techenie svobodno rasshiriaiushchegosia gaza s ploskoi perexodnoi poverkhnost'iu (Axisymmetric supersonic flow of a freely expanding gas with a plane transition surface). *Collection of Computing Mathematics* No. 2. Izd-vo. Akad. Nauk SSSR, 1957.

Translated by M.V.D.